SPE/DOE 27811

Miscible Or Near Miscible Gas Injection - Which is Better?

F.B. Thomas*, Nancy Holowach, XueLong Zhou*, D.B. Bennion, and D.W. Bennion*
Hycal Energy Research Laboratories Ltd.

*SPE Members

This paper was prepared for presentation at the SPE/DOE Ninth Symposium on Improved Oil Recovery held in Tulsa, Oklahoma, U.S.A., 17-20 April 1994.

INTRODUCTION

Miscible flooding was invented many years ago, and in the 1950's it was viewed as one of the most promising techniques to use for improving oil recovery from a reservoir.[1,2,3,4,5,6,7] Since that time many groups have researched what would be the most important parameters to optimize in the lab, have developed theoretical models to correlate these parameters, and then have implemented these "optimally designed" gas injection systems in the field. Amidst all the increase in technology and sophistication there is still ongoing debate as to whether one needs to achieve miscibility in order to optimize the recovery or whether a degree of immiscibility, characterized by the name "near miscible", is equally adequate for field implementation in enhanced oil recovery processes.

This paper seeks to provide insight into these questions by reviewing some of the parameters which are at work in gas injection EOR as well as qualifying some of the techniques which can be used in designing gases for injection. Moreover, case histories are described herein where laboratory work was performed, phase behavior described, and then the gas injected into the reservoir. Results from the field are then shown and commentary included on the field performance.

References and illustrations at end of paper

BACKGROUND

Gas injection for EOR is a very mature discipline applied throughout the world. Depending upon where in the world one is implementing gas injection and to whom one is speaking the post-mortem evaluations of "miscible flooding" may vary from being very successful to "miserable flooding". The reason for some floods being very successful and others less so may be as closely tied to how one measures the parameters of gas injection as to the nature of the process itself. In order to discuss the specifics of "miscible flooding" one needs to initially discuss the variables which are involved in the process. It is impossible to comment on all of these factors so only three will be referred to.

Most importantly, the geology enters into the basis for successful gas injection processes. It is very difficult to have a successful process when the geology is inconsistent with that which one is trying to accomplish. The effects due to geology can be divided up into macroscale and microscale parameters.

From a macroscale standpoint one encounters macroscale influences whenever one has different flow units in a reservoir. These heterogeneities may seriously impact the way fluids flow. For example, there are case histories where a horizontal impermeable barrier has been penetrated by a vertical fracture, caused by excessive injection pressures, or a previous hydraulic fracture treatment thus resulting in extremely poor flood performance. In such examples, no matter how well the fluid phase behavior was designed, macroscale influences may oftimes sabotage the outcome, even on a well-designed gas injection scheme.

Macroscale details such as these need to be addressed ab initio and cannot be ignored. In these cases, profile modification may be the only way to enhance recovery from a reservoir dominated by such macroscale effects. For the most part, however, one always has some macroscale heterogeneity to work with, but one can normally evaluate the effect and character of such by routine reservoir characterization studies and include them in one's conceptual framework when designing the flood.

Microscale influences, on the other hand, are sometimes omitted in designing a gas injection process. Microscale details are referred to in Figure 1, for example, where one observes the pore size distribution and the relative importance of the different pore sizes evaluated on this basis. In such a case one sees that pore throats range from less than 1 micron up to 130 microns. This pore size distribution can impact significantly the optimal design. Techniques for evaluating the pore size distribution are familiar to the reader and examples of this are mercury capillary pressure testing as well as petrographic image analysis (PIA). How these microscale influences connect to the overall design depends upon the interaction between two parameters. These parameters are interfacial tension and viscosity ratio.

Interfacial Tension

Interfacial tension plays an important role in "miscible flooding" because it is the most sensitive and most easily modified variable in the capillary number. Gupta[8] shows a standard set of desaturation curves as a function of capillary number. Flow velocity, viscosity and interfacial tension define the value of the capillary number. Orders of magnitude change in capillary number are normally required to result in significant decreases in residual oil saturation and therefore means of altering these variables have been developed. With gas injection one can obtain a significant decrease in interfacial tension by injecting gases at appropriate pressures and composition into the reservoir; in-situ mass transfer dictates the level of IFT reduction. Considerable decrease in IFT (at relatively low cost) is the benefit of miscible flooding. To achieve even one order of magnitude increase in capillary number by increasing velocity or viscosity is much more difficult and costly. The potential to reduce IFT is the reason for which much effort is concentrated on the phase behavior associated with gas injection projects.

The reason interfacial tension plays such a dominant role in the recovery of oil is well documented in the literature[9] and will not be detailed herein. The reduction in capillary pressure due to the decrease in IFT results in the gas being able to access pore throats which were essentially isolated from the flowing gas phase at a higher interfacial tension level. This influence has been discussed in the context of the Laplace equation

$$P_{cap} = \frac{2\sigma \cos \phi}{r} \qquad (1)$$

This reduction in capillary forces between the oil and the injection gas results in more efficient sweep and reduced residual oil saturation (So_r).

Viscosity Ratio

Simultaneously with the injection of low interfacial tension gases one also has a destabilizing influence which is associated with the very adverse viscosity ratio. The endpoint relative permeabilities to oil and gas are usually of the same order of magnitude. However, typical oil and gas viscosity ratios can range from a minimum of 5 up to 10,000. Since the tendency to flow is inversely proportional to the viscosity, an applied differential pressure results in preferential gas flow. This results in the characteristic viscous fingering which is so prominent in the EOR literature.[10,11,12] A compromise is therefore established between mobility and IFT depending upon the micro and macroscale geological characteristics in which the fluids flow. This interaction needs to be accounted for when performing the experimentation as well as the field implementation. The next section addresses techniques used to determine the optimal design for gas injection.

EVALUATION OF WHAT IS THE OPTIMAL GAS

Knowing that the parameters discussed previously enter into the optimization of the gas injection process, the experimental program must therefore give consideration to geology, interfacial tension influences, as well as mobility characteristics. Many evaluations of miscibility were, and continue to be, made based upon a displacement efficiency criterion normally associated with a synthetic porous medium[13,14] (slim tube tests) wherein a series of glass beads or artificial sand pack is saturated with reservoir fluid. The prospective gas composition and pressure is then used to displace the reservoir fluid from the porous medium. One usually observes a recovery vs pressure plot, such as associated with Figure 2, wherein an increase in pressure results in insignificant incremental oil production. In such a situation the values of interfacial tension and mobility are reasonably represented, but the microscale influences of the geology are often neglected since the porous medium is not representative of the reservoir. From the previous discussion of capillary pressure phenomena the displacement efficiency may be representative of this synthetic pore size distribution but may be far removed from the type of recovery which one will observe in the reservoir rock. For example, Mungan[15] has described the difference between the "minimum miscibility pressure" (MMP) using a synthetic porous media and the "MMP" associated with using reservoir rock. In that case the difference was more than 12.5% (250 psi), the reservoir rock indicating the higher MMP.

Therefore the criterion of displacement efficiency in a synthetic porous medium is only a convention and not an indication of miscibility. This is consistent when one refers this to the discussion on pore size distribution such as that in Figure 1 and how the interfacial tension interacts with that pore size distribution. One can observe that if 100% recovery is desired, then one must achieve the situation where the interfacial tension reaches zero (from equation 1). This is the definition of miscibility that is used herein, that is, the development of a zero interfacial tension zone.

By interpolation therefore one would classify the discontinuity on a recovery-pressure (or enrichment) plot as the conditions consistent with a threshold IFT value. IFT values above this contribute to bypassed oil and impact the recovery. IFT values below the threshold may contact more of the small pore throats but if there are very few of them in the slim tube, then little or no influence will be observed. The same may not be the case in the reservoir rock and thus the potential problem associated with a convention such as 95% recovery in a slim tube. Unless the porous medium used is representative reservoir rock the displacement criterion for classifying acceptable IFT levels may not be adequate. Figure 3 presents a schematic representation of this.

Therefore, measurement of the IFT response is recommended rather than basing a design upon a subjective displacement criterion. Of course an MMP plot could also be performed using reservoir rock but to generate at least four points on the MMP plot would be much more costly than to explicitly measure IFT. In doing so a discrete series of gas and reservoir fluid mixtures are synthesized corresponding to the phase behavior mechanisms which are at work in the system and the compositional paths and equilibrium compositions analyzed. In many cases the compositional paths followed by these discrete contacts are not comparable to the compositional paths associated with the dynamic displacements. However the gas and liquid equilibrium compositions are oftimes very comparable, as is shown in Figure 4. Most commonly these compositional phase loops have been used to assess what level of miscibility is being achieved.

Zick[16] Novosad[17] and Dindoruk[18] have shown that the ternary diagram tie-line extrapolation techniques are often erroneous in their estimation of miscibility limits. Multicontact procedures are not recommended for ternary diagram extrapolation techniques, but they can be extremely useful to quantify IFT reduction as a function of contact number. In these cases one can see not only whether a zero IFT zone is achieved, but how close to miscibility one has approached and then use those equilibrium fluids to identify the effect of that IFT change by performing a fluid flow test.

Confirmation of the departure of the asymptotic fluids from miscibility pressure can be quantified. For example, based upon the fluids observed in Figure 4, one can use the upper phase from the limiting tieline (forward contact) and contact that with reservoir fluid in different concentrations, thus generating a pressure-composition diagram (termed a multicontact P-x diagram). Figure 5 describes a conventional pressure-composition relationship as well as a series of multicontact pressure-composition diagrams. One can see an extreme dependence of critical pressure and cricondenbar as a function of contact number. This information allows quantification of the approach to miscibility and even though the compositional path may be different from that followed in a dynamic system, the equilibrium compositions, and therefore the interfacial tensions, should be representative.

More recently the Rising Bubble Apparatus developed by Christianson and Kim[19] has also provided insight into miscible behavior. Thomas et al[20] have provided a comparative study based upon six oils which they analyzed comparing the RBA and these other techniques. Their findings indicated:

1. For five out of the six oil-solvent systems that were investigated, the MMP RBA was normally within 300 psi of the MMP determined from the slim tube.

2. In four of six cases the MMP_{RBA} was higher than the $MMP_{slim\ tube}$. From this sample set, the MMP RBA would, in general, be conservative compared to slim tube testing.

3. The MMP associated with multicontact testing would normally be expected to be more conservative than the RBA. ($MMP_{MC} > MMP_{RBA} \geq MMP_{slim\ tube}$).

The literature[20,21] provides evidence that the RBA is useful for scoping studies because it is extremely efficient and approximately 1 order of magnitude less expensive than detailed slim tube testing. The drawbacks are that the RBA is limited because it provides very little quantitative data (compositions, densities, IFT) and there is a degree of subjectivity, particularly for those systems where the bubble disappearance, due to IFT change, is difficult to see.

These techniques (slim tubes, multicontact tests and RBA) have been used extensively by the authors and normally provide, in conjunction with the microscale geology and in light of the reservoir character, a very good idea of what the optimal IFT design is. The RBA provides an approximate MMP value within one or two days followed by a slim tube test which comprises the necessary condition for solvent design from an IFT perspective. That is, the slim tube test must exhibit very efficient displacement in order for the solvent to be acceptable from an IFT perspective; however a highly efficient slim tube does not necessarily equate to an adequate IFT reduction suitable for the reservoir. Subsequent to the satisfactory performance of the slim tube, a starting point is available for more detailed investigation into pressure and injection gas composition. Multiple contacts are then performed whereby IFT and viscosity reductions are quantified along with equilibrium compositions. An EOS model is then used to fit the data arising from this testing (densities, viscosities, IFT, compositions, gas/liquid saturations, critical point migration as a function of contact number) and then input to a compositional simulator for insight into dynamic systems. What remains is to couple the phase behavior to the way it will flow in the reservoir rock.

Evaluation of Mobility vs IFT

The previous section described how the optimization with respect to interfacial tension is performed. The influence of interfacial tension in the presence of the reservoir's pore size distribution and the fluids' mobilities needs to be evaluated. To do this the fluids which have been developed as part of the multicontact procedure, such as that in Figure 4, are chosen for the generation of the fractional flow curves. In most cases one sees a very early breakthrough with the fluids produced from contacting in the manner opposed to the natural mechanism exhibited by the fluids. That is, for a system dominated by extraction, a series of reverse contacts (where continued solvent is added to the equilibrium liquid from the previous flash) results in an increase in IFT and also a slight increase in the viscosity ratio between the gas and liquid. On the other hand, by performing contacts in a manner consistent with the mechanism exhibited by the fluids themselves one sees a decrease in IFT and normally an improvement in mobility ratio.

Depending on the system, the reduction in oil viscosity due to gas injection can sometimes be equally as important as IFT reduction. The decrease in IFT is frequently measured in orders of magnitude whereas the change in viscosity between the fluids is usually measured at less than a factor of 8 - 10 times (CO_2 systems and high C_{3+} solvent sometimes being an exception). For some systems, as is shown in Figure 6, a decrease in IFT results in a small increase in recovered oil. In other cases, however, as is shown in Figure 7, a decrease in IFT results in a substantial decrease in residual oil saturation caused by accessing most of the pores containing oil. The important feature of this testing is that it allows for the evaluation of the potential benefit of IFT reduction in the presence of realistic mobility ratios. Typical unsteady state gas/oil relative permeability experiments do not span the range of interfacial tensions which would be present in a mass transfer-dominated system and are inadequate in assessing the mobility/IFT interaction. Thus typically, the coupling of IFT, mobility and pore size distribution is omitted from analysis. However, if one performs K_{rel} testing such as proposed herein, one has quantified the influence of IFT reduction in the context of the reservoir character and in a much less expensive and in a more controlled manner than with a full length stacked core flood. If the system responds more as Figure 6, then one may be more concerned with controlling mobility than with the IFT decrease. If on the other hand, one sees an effect such as Figure 7, then effort for IFT optimization would be justified.

CASE STUDIES

The previous sections have treated the elements of an experimental program in order to evaluate IFT and mobility influences in the presence of the reservoir's porous media. A number of studies have been performed such as this wherein the laboratory testing has indicated that very efficient gas injection processes should be possible. Case studies are now discussed.

Oil-Solvent System No. 1

The oil that was used in this evaluation was a very light oil of approximately 50 - 55° API with a GOR of approximately 370 m^3/m^3 (2077 scf/b). The reservoir temperature was 99°C (210°F) and the bubblepoint of the oil was 19 167 kPa (2780 psig). The injection gas which was targeted for injection is shown in Table 1. A series of slim tube runs was then performed along with an RBA test using this oil. The MMP_{RBA} and the $MMP_{slim\ tube}$ compared very closely at 3200 psi (±0.60%). Multiple contacts were then performed with this fluid at 3200 psi. After four contacts there was no further change in the upper phase composition as a result of forward contacts. The phase compositions are shown in Table 2. Although the interfacial tension was decreasing with contacts at MMP_{RBA} ($MMP_{slim\ tube}$) the presence of two phases was still obvious, corresponding to non zero interfacial tension. The upper phase resulting from this series of four forward contacts was then combined with the reservoir fluid and a pressure composition diagram generated.

Figure 8 describes the P-x diagram done in a conventional manner as well as the pressure composition diagram performed with the asymptotic upper phase from these forward contacts. The cricondenbar associated with multicontact pressure composition diagram was approximately 350 psi higher than the MMP_{RBA} and $MMP_{slim\ tube}$. Moreover, the level of IFT reduction was also approximated using one measured interfacial tension and then using the parachor correlation to predict the other interfacial tensions based upon the compositional analyses of the fluids. Budgetary constraints prohibited the inclusion of constant interfacial tension/relative permeability work at upper and lower IFT limits, but it was anticipated that due to the very small viscosity ratio, approximately 5 (0.10/0.02) the mobility, although being important would not be as dominant as in other systems and that the interfacial tension reduction would play a major role.

The fact that the mobility ratio was fairly low justified the concentration upon reducing interfacial tension and particularly in light of the fact that the core was very oil-wet and contained only 3% initial water saturation. This implies that the oil would be present in even the smallest pores of the rock and in order to access all of the potential oil a zero interfacial tension zone would be recommended. Had the core been water-wet, operation at MMP would have been less important, particularly if the water saturation was associated with the smallest pore throats. In that case the IFT of the gas-oil would only have to be low enough to recover oil from all of the oil filled pores ignoring those pores which are filled with water. Wettability can impact solvent design from this perspective.

Miscible flooding was then implemented in the field and has been reported in a number of references.[22,23,24] Figure 9 shows a map of the Brassey reservoir and the specific wells which are present in this system. The solvent which was injected into this reservoir was approximately 10% richer in C_{2+} content than the solvent which was used in the generation of the pressure composition diagram as well as the multicontact P-x diagram shown in Figure 8. In addition, the reservoir was initially highly undersaturated with a discovery pressure of approximately 5800 psi and the reservoir pressure was never allowed to drop below 4000 psi. Therefore in light of the response of Figure 8 one knows that the gas was always multicontact miscible and most probably first contact miscible.[25] The field implementation is performing well but breakthrough is occurring in all but one of the producing wells. The recovery is approximately 30% of the original oil in place at time of writing.

When breakthrough occurred in wells D44F and C23F, investigation was made to ascertain whether the high GOR's observed were associated with a single phase flowing in situ. To determine whether the system is single or two-phase downhole from a conventional P-x diagram one would conclude that a GOR of approximately 900 m^3/m^3 would indicate a two-phase system. However, in the field the pressure will never rise above the reservoir pressure and therefore much of the data obtained from the conventional P-x diagram lies above what is a possible operating pressure. Points on the multicontact P-x diagram (Figure 8) had GOR's up to 1000 m^3/m^3 and the GOR from a bottomhole sample in well D-44F was approximately 900 m^3/m^3. At the pressure of the cricondenbar of the multicontact P-x of Figure 8 the system was single phase and since the pressure in the reservoir had never been depleted below 4000 psi the produced fluid corresponded to a single phase in situ. The compositional comparison between the BHS and the fluid from the MCP-x diagram's 6th addition is shown in Table 3. The question then remains was the fluid associated with the leading edge of the displacement after which the transition zone and the injection gas would break through, or was it associated with a bypassing gas which was vaporizing a sufficient amount of oil and thus creating a very rich gas. The system corresponded to a dewpoint and is thought to be indicative of a bypassing gas which is dragging an amount of oil with it. Figure 10 shows the comparison between BHS, the live oil and the MCP-X composition. The compositions have been renormalized in the C_{5+} components. If the liquids were to be produced by vaporization of oil as the gas passed by, it would be improbable that the distribution of C_{6+} components would be similar to the oil. This was interesting in light of the fact that the displacement is thought to be first contact miscible. If any EOR scheme should not result in bypassing, it would be expected to be FCM.

Neglecting any macroscale heterogeneity discussion which does not appear to be existent in this reservoir, according to company personnel, could microscale details result in possible bypassing, particularly for an FCM displacement? Work has been done on systems such as these and even though a single phase is associated, many times an effective viscous finger can be produced; the mobility ratio resulting from the contacting of the oil and the gas tends to propagate and follow the path of least resistance. Figure 1 showed a sample pore size distribution generated from a mercury injection test. It is possible that the fluid preferentially flows through the larger pore throats even though it potentially has access to all of the pore throats from an IFT perspective.

In conclusion, therefore the result of the solvent design from the laboratory indicated that a very efficient displacement should be possible in the field because of the necessary condition of low interfacial tension was being achieved in the presence of a small adverse mobility ratio. The field results show that efficient displacement was achieved and with respect to a horizontal displacement such as this, 25 - 30% recovery at this point in the flood is classified as being successful both technically and economically. Relaxing the IFT criterion on this system would be expected to have had deleterious impact on field performance.

Case History No. 2

This reservoir system is comprised of a very large area containing hundreds of millions of barrels of oil in place with an API gravity of approximately 40°. The experimental work on this reservoir system included many slim tube tests performed over a ten year period. The discontinuities were generated from a series of four slim tube tests at different combinations of C_{2+}% and C_{2+} MW. Figure 11 shows an example of this type of relationship. To produce this figure three series of slim tube tests were done wherein a MW of the C_{2+} fraction in the injection gas was specified and then a recovery vs enrichment plot was generated for each MW level. The correlation of Figure 11 was comprised of more than 12 slim tube tests which could have been performed much more efficiently with more recent techniques (RBA, IFT measurements). Years after this correlation was developed the same fluids were then subjected to analysis using more specific testing techniques and the correlation was known to exhibit finite IFT values and the actual MMP was higher than that suggested by Figure 11. One of the more important parameters which was observed, however, was that the slim tube performance achieved with the high ethane content gas was comparable to the injection gases containing more C_{3+} (higher C_{2+} MW). The recoveries were very comparable - 95.0 and 95.1% for low and high MW C_{2+} respectively.

Coreflooding was also performed using the solvent designs available from the slim tube work and the corefloods varied in efficiency between 75 and 95% depending upon the pressure and solvent composition. The coreflooding indicated more favorable results from the higher C_{2+} MW however. The compromise between the IFT and mobility in the actual porous medium showed that for the same IFT level (and none of the compositions from Figure 11 corresponded to a zero IFT zone) the **rate of recovery** was superior with the higher MW C_{2+} fraction. It is thought that this would be due to a greater affinity of the C_{3+} in the heavier C_{2+} fraction to dissolve in the oil compared to the higher ethane content fluids. This results in lower oil viscosity than with the ethane-based C_{2+}. For formations with very small pore throat diameters it is thought that the difference between these two gases may be less distinct. However, where larger pore throats are present, the level of viscosity reduction may even override the contribution from IFT decrease. The fact that the rate of recovery was altered by the C_{2+} MW could possibly impact payout period considerations for pilot and field-scale design. The gas selected was an ethane-rich solvent containing as much as 75-80% ethane. The flood to date has performed in a manner ranging from fairly efficient to relatively poor depending upon the zone as well as variations in thickness and reservoir quality. As the injection gas increased in C_{2+} MW the field performance seemed to improve even though the IFT criterion based on the slim tube testing did not presage such.

Another interesting feature of this system was derived from tracer studies which were performed. Figure 12 shows the different tracer profiles from the field-scale tracers which were performed in this study. Since the system corresponded to a tertiary implementation, once gas began to be injected the solvent was spiked with tritiated ethane. From Figure 12 one can see that the tritiated ethane migrated in an easterly manner from one of the injection wells to the producers. Following the slug of gas which was injected, more water was injected into the formation and the water traveled in a more southerly direction. This overall area (east and south zones) of the reservoir was deemed to be successful from a recovery standpoint; however the bulk of the oil recovered is thought to be due to secondary-gas recovery as opposed to tertiary gas injection. A scenario such as this could be explained from an interfacial tension, mobility and pore size distribution perspective. It is thought that there would be a general trend in properties of the reservoir, different to the east than to the south.

The viscosity of the oil and the water were comparable (0.4 cP oil and 0.30 cP water) thus resulting in a viscosity ratio of the same order of magnitude between the water-gas and the oil and gas. It is therefore thought that the reason for which the gas migrated predominantly in a manner perpendicular to the water was due to an IFT influence wherein the oil filled pore throats were contacted more effectively and more easily by the gas due to a much lower interfacial tension. Once these pore throats were contacted, then subsequent gas continued to follow where the previous gas saturation had been established thus resulting in an almost exclusive uni-directional gas pattern. Once water was begun it would have followed the paths which had been previously established by the waterflooding. Water flow in the southern direction could be caused by the presence of higher pore throat sizes in a southerly direction. Since the water could not enter into the tighter pores to the east of the injector, due to an IFT criterion, it could only flow south. Once the water began to flow then subsequent water injection would have followed in the same direction. For such a case the only way to enhance the recovery would be to implement profile modification strategies wherein the larger pore throats, which are now dominated by mobility effects, are essentially reduced in their ability to transport injection fluids, thus enabling the lower IFT fluids, specifically the injection gas, to contact those zones which previously have not been gas flooded.

In a system such as this, had lab work been performed which included evaluation of mobility versus IFT effects, one may have been aware of such potentialities. By analogy, once the interfacial tension has determined which pore throats are available for flow, the mobility effects then govern how quickly the fluids flow within those available pore throats. There is some evidence which would indicate that even though the permeability of such a system may be comparable in both directions, if the pore throat sizes are larger but fewer (smaller coordination number) then the fluid can flow in that rock.[26] Mobility effects may dominate in these systems. Conversely for the same permeability rock, if the pore throats are more numerous (larger coordination number) but smaller in diameter then even though the permeability is the same, the lower IFT fluid will be the only one to be able to enter into that zone. Therefore along with permeability the pore size distribution associated with the reservoir can determine the effects such as shown in Figure 12.

SUMMARY

In light of the work performed by the authors as well as a review of many public and private domain gas injection studies, the following highlights can be observed:

1. Historically, many systems which were designed as miscible floods would be better described as near miscible, depending on the technique used to evaluate them.

2. Many laboratory tests and some field implementations have indicated that near miscible and miscible injection gases perform in a comparable manner. These, however, are influenced by a number of properties.

    - The relative pore size distribution wherein if the core exhibits predominantly very small pore throats and has a very small standard deviation, then interfacial tension optimization will be important.

    - If the pore size distribution is more broad, exhibiting a larger range of pore throat sizes, then viscosity influences will often dominate.

    - In some cases to design an injection gas to develop a zero interfacial tension zone would be overkill, particularly for those systems which are water-wet and where the smaller pore throats are filled with water.

    - For those systems which exhibit larger pore throat sizes, IFT optimization may be less crucial to performance than viscosity reduction. In these cases solubility of gaseous components will play a much more major role for the same level of interfacial tension due to their impact on viscosity.

3. Laboratory testing should account for the interaction between viscosity, IFT, and pore size distribution rather than concentrating only upon the assessment of what is miscible. That is, the quantification of IFT reduction and how that IFT reduction interacts with mobility in the pore size distribution is important to measure.

4. Low IFT is a necessary condition for efficient recovery from most reservoirs, but in many cases zero IFT is unnecessary unless the pore throat size distribution is extremely tight and the rock is oil-wet.

NOMENCLATURE AND ABBREVIATIONS

Pcap - capillary pressure
σ - interfacial tension (IFT)
cos ϕ - cosine of contact angle
r - radius of pore throat
So_r - residual oil saturation
MMP - minimum miscibility pressure
MMP_{RBA} - MMP from Rising Bubble Apparatus
$MMP_{slim\ tube}$ - MMP from slim tube testing
MMP_{MC} - MMP from multicontact experiments

REFERENCES

1. Koch, H.A. Jr., "High Pressure Gas Injection Is A Success:, World Oil, (Oct 1956), 143 p. 260.

2. Hall, H.N. and Geffen, T.M.: "A Laboratory Study of Solvent Flooding", Trans AIME, (1957) 210, pp. 48-57.

3. Whorton, L.P. and Kieschnick, W.F.: "Oil Recovery By High Pressure Gas Injection", Oil & Gas Journal, (April 6, 1950) p. 78.

4. Whorton, L.P. et al, U.S. Patent No. 2623596, Dec. 30, 1952.

5. Whorton, L.P. and Brownscombe, E.R., U.S. Patent No. 2724437, Nov. 26, 1955.

6. Stone, H.L. and Crump, J.S.: "The Effect of Gas Composition Upon Oil Recovery by Gas", TRANS AIME (1956) Vol. 207, p. 105.

7. Kehn, D.M., Pyndus, G.T. and Gaskell, M.H.: "Laboratory Evaluation of Prospective Enriched Gas Drive Projects", JPT (June 1958, pp. 45-58.

8. Gupta, T.: Micelar Flooding - Compositional Effects on Oil Displacement", SPE (1979) SPE #7063.

9. Stalkup, F.I.: "Miscible Flooding", SPE Monograph, 1984.

10. Collins, R.E.: Flow of Fluids Through Porous Media, Reinhold Publishing Co., New York City (1961) 201.

11. Gardner, J.W. and Ypma, J.G.J.: "An Investigation of Phase Behavior-Macroscopic Bypassing Interaction in CO_2 Flooding", paper SPE 10686 presented at the 1982 SPE/DOE Symposium on Enhanced oil Recovery, Tulsa, April 4-7.

12. Habermann, B.: "The Efficiencies of Miscible Displacement as a Function of Mobility Ratio", Trans AIME (1960) 219, 265-272; Miscible Processes, Reprint Series, SPE, Dallas (1965) 8, 106-14.

13. Randall, T.E. and Bennion, D.B.: "Laboratory Factors Influencing Slim Tube Test Results", JCPT, (July-Aug. 1989), Vol. 28, No. 4, pp. 60-70.

14. Flock, D.L. and Nouar, A., "Parametric Analysis on the determination of the Minimum Miscibility Pressure in slim Tube Displacements; Hycal Energy Research Laboratories Ltd. JCPT, (Sept-Oct 1984) pp 80-88.

15. Mungan, N: "An Evaluation of CO_2 Flooding", presented at SPE Western Regional Meeting held in Long Beach, California, March 20-22, 1991.

16. Zick, A.: "A combined Condensing, Vaporizing Mechanism in Displacement of Oil by Enriched Gases", SPE Paper #15493, SPE Fall Meeting, New Orleans, 1986.

17. Novosad, Z.: "On the Aspects of Reservoir Fluids Phase Behavior Important in Design of Miscible Gas Injection Processes", IOR Symposium, Stavanger, Norway, May 21-23, 1991.

18. Dindoruk, B: "Analytical Theory of Multiphase, Multicomponent Displacement in Porous Media; PH.D. dissertation, Stanford University, CA, 1992.

19. Christiansen, R.L. and Kim, H: "Apparatus and Method for Determining the Minimum Miscibility Pressure of a Gas in a Liquid", Canadian patent 1 253 358.

20. Thomas, F.B., Zhou, X.L., Bennion, D.B. and Bennion, D.W.: A Comparative Study of RBA, P-X, Multicontact and Slim Tube Results, JCPT, Volume 33, No. 2 (February 1994) pp. 17-26.

21. Elsharkawy, A.M., Poettmann, F.H. and Christiansen, R.L.: "Measuring Minimum Miscibility Pressure: Slim Tube or Rising Bubble Method, SPE 24114.

22. Woofter, D.M. and MacGillivray, J.: "Brassey Canada: Development of an Aeolian Sand - A Team Approach", SPERE, (May 1992) p. 165-172.

23. Whitten, M.D., Anderson, J.H., Tinker, C.E.: "Miscible Flood From Inception: The Brassey Field Development, British Columbia, Canada", paper SPE 19655 presented at the 64th Annual Technical Conference of the SPE, San Antonio, October 8-11, 1989.

24. Anderson, J.H., Laurie, R.A., Loder, W.R., Kennedy, P.: "Brassey Field Miscible Flood Management Program Features Innovative Tracer Injection", Paper SPE 24874 presented at the 67th Annual Technical Conference of the SPE, Washington, D.C., October 4-7, 1992.

25. Rossall, J.W. and Gurpinar, O.M.: "A Compositional Simulation Evaluation of the Brassey Artex B Pool, British Columbia, Canada", SPE Meeting, Houston TX, Oct. 3-6, 1993, SPE 26404.

26. Thomas, Mark B.: Personal communication February 8, 1994.

TABLE 1
COMPOSITION OF OIL-SOLVENT SYSTEM 1

Component	Oil Composition Recombined Fraction	Solvent
N_2	0.0073	0.0059
CO_2	0.0020	0.0051
H_2S	0.0000	--
C_1	0.4481	0.8770
C_2	0.1026	0.0622
C_3	0.0760	0.0333
i-C_4	0.0239	0.0086
n-C_4	0.0379	0.0080
i-C_5	0.0205	-
n-C_5	0.0219	-
C_6	0.0350	-
C_7	0.0243	-
C_8	0.0315	-
C_9	0.0189	-
C_{10}	0.0221	-
C_{11}	0.0170	-
C_{12}	0.0134	-
C_{13}	0.0120	-
C_{14}	0.0088	-
C_{15}	0.0071	-
C_{16}	0.0048	-
C_{17}	0.0035	-
C_{18}	0.0033	-
C_{19}	0.0028	-
C_{20}	0.0021	-
C_{21}	0.0016	-
C_{22}	0.0011	-
C_{23}	0.0011	-
C_{24}	0.0009	-
C_{25}	0.0006	-
C_{26}	0.0006	-
C_{27}	0.0005	-
C_{28}	0.0005	-
C_{29}	0.0005	-
C_{30+}	0.0010	-
CycloC_5	0.0024	-
MCycloC_5	0.0043	-
Benzene	0.0022	-
CycloC_6	0.0035	-
MCycloC_6	0.0096	-
Toluene	0.0060	-
o-Xylene	0.0029	-
1,2,4-Trimethylbenzene	0.0019	--
EB/MP-Xylene	0.0117	
Molecular Weight	56.1	18.76
GOR (cc/cc)	364.1	
Ppc kPa (psig)	19167 (2780) @ 99°C	
Ppc kPa (psia)		4590 (665.7)
Tpc (K)		207.1
Mole Fraction C_{6+}	0.2598	
MW C_{6+}	137.8	
Density C_{6+}	0.789	
Corrected for CO_2 content in the solvent		

TABLE 2
MULTICONTACT PHASE COMPOSITION SUMMARY

Component	Live Oil	Equilibrium Liquids					Equilibrium Vapours			
		1st	2nd	3rd	4th	Solvent	1st	2nd	3rd	4th
N_2	0.0090	0.0055	0.0071	0.0104	0.0154	0.0059	0.0109	0.0119	0.0142	0.0206
CO_2	0.0032	0.0145	0.0022	0.0017	0.0017	0.0051	0.0058	0.0032	0.0025	0.0033
H_2S	0.0000	0.0000	0.0000	0.0000	0.0000	0.0000	0.0000	0.0000	0.0000	0.0000
C_1	0.4578	0.4990	0.5344	0.5355	0.5461	0.8770	0.8071	0.7247	0.7023	0.6902
C_2	0.1019	0.0791	0.0884	0.0933	0.0936	0.0622	0.0844	0.0932	0.0930	0.0926
C_3	0.0749	0.0607	0.0632	0.0681	0.0668	0.0333	0.0485	0.0561	0.0577	0.0575
i-C_4	0.0234	0.0199	0.0196	0.0202	0.0204	0.0086	0.0125	0.0150	0.0158	0.0156
n-C_4	0.0369	0.0301	0.0305	0.0308	0.0314	0.0080	0.0161	0.0211	0.0226	0.0224
i-C_5	0.0200	0.0150	0.0165	0.0161	0.0163	0.0000	0.0051	0.0091	0.0102	0.0105
n-C_5	0.0215	0.0165	0.0177	0.0169	0.0170	0.0000	0.0046	0.0090	0.0100	0.0104
C_6	0.0331	0.0266	0.0288	0.0270	0.0270	0.0000	0.0048	0.0135	0.0157	0.0171
C_7	0.0246	0.0216	0.0201	0.0200	0.0182	0.0000	0.0000	0.0060	0.0074	0.0082
C_8	0.0316	0.0293	0.0262	0.0262	0.0233	0.0000	0.0000	0.0075	0.0094	0.0125
C_9	0.0188	0.0183	0.0158	0.0157	0.0139	0.0000	0.0000	0.0042	0.0055	0.0058
C_{10}	0.0217	0.0223	0.0184	0.0180	0.0161	0.0000	0.0000	0.0044	0.0061	0.0062
C_{11}	0.0167	0.0180	0.0147	0.0137	0.0127	0.0000	0.0000	0.0032	0.0044	0.0045
C_{12}	0.0128	0.0145	0.0111	0.0107	0.0096	0.0000	0.0000	0.0021	0.0030	0.0031
C_{13}	0.0111	0.0136	0.0102	0.0094	0.0085	0.0000	0.0000	0.0018	0.0025	0.0025
C_{14}	0.0080	0.0099	0.0074	0.0066	0.0060	0.0000	0.0000	0.0011	0.0015	0.0016
C_{15}	0.0065	0.0082	0.0061	0.0054	0.0049	0.0000	0.0000	0.0009	0.0012	0.0012
C_{16}	0.0042	0.0057	0.0042	0.0037	0.0034	0.0000	0.0000	0.0005	0.0007	0.0007
C_{17}	0.0033	0.0049	0.0034	0.0027	0.0026	0.0000	0.0000	0.0004	0.0005	0.0005
C_{18}	0.0028	0.0042	0.0029	0.0022	0.0021	0.0000	0.0000	0.0003	0.0004	0.0004
C_{19}	0.0020	2.0035	0.0021	0.0018	0.0016	0.0000	0.0000	0.0002	0.0003	0.0003
C_{20}	0.0014	0.0028	0.0019	0.0014	0.0014	0.0000	0.0000	0.0001	0.0002	0.0002
C_{21}	0.0011	0.0021	0.0014	0.0010	0.0010	0.0000	0.0000	0.0001	0.0001	0.0001
C_{22}	0.0009	0.0019	0.0011	0.0008	0.0008	0.0000	0.0000	0.0001	0.0001	0.0001
C_{23}	0.0008	0.0015	0.0010	0.0006	0.0006	0.0000	0.0000	0.0001	0.0001	0.0001
C_{24}	0.0008	0.0013	0.0009	0.0006	0.0006	0.0000	0.0000	0.0000	0.0001	0.0001
C_{25}	0.0006	0.0012	0.0008	0.0005	0.0006	0.0000	0.0000	0.0000	0.0000	0.0001
C_{26}	0.0006	0.0010	0.0007	0.0004	0.0005	0.0000	0.0000	0.0001	0.0000	0.0001
C_{27}	0.0006	0.0009	0.0006	0.0004	0.0004	0.0000	0.0000	0.0000	0.0001	0.0001
C_{28}	0.0005	0.0010	0.0006	0.0003	0.0005	0.0000	0.0000	0.0000	0.0000	0.0001
C_{29}	0.0005	0.0008	0.0006	0.0003	0.0004	0.0000	0.0000	0.0000	0.0000	0.0000
C_{30+}	0.0011	0.0018	0.0013	0.0007	0.0008	0.0000	0.0000	0.0002	0.0001	0.0002
$CycloC_5$	0.0025	0.0022	0.0021	0.0019	0.0019	0.0000	0.0000	0.0005	0.0006	0.0007
$MCycloC_5$	0.0044	0.0039	0.0036	0.0035	0.0033	0.0000	0.0000	0.0010	0.0012	0.0014
Benzene	0.0023	0.0021	0.0019	0.0018	0.0017	0.0000	0.0000	0.0005	0.0006	0.0007
$CycloC_6$	0.0036	0.0033	0.0030	0.0029	0.0027	0.0000	0.0000	0.0008	0.0010	0.0011
$MCycloC_6$	0.0098	0.0090	0.0081	0.0080	0.0072	0.0000	0.0000	0.0022	0.0027	0.0004
Toluene	0.0061	0.0057	0.0053	0.0051	0.0045	0.0000	0.0000	0.0014	0.0017	0.0019
o-Xylene	0.0029	0.0029	0.0025	0.0024	0.0022	0.0000	0.0000	0.0006	0.0008	0.0009
1,2,4-Trimeth	0.0019	0.0020	0.0017	0.0016	0.0015	0.0000	0.0000	0.0004	0.0005	0.0006
EB/MP-Xylene	0.0117	0.0115	0.0099	0.0098	0.0087	0.0000	0.0000	0.0026	0.0034	0.0036
MW Recombined Oil	54.62	57.32	50.58	48.08	46.51	18.76	20.97	27.62	29.51	30.19
MW Separator Oil	128.40	138.72	132.80	129.18	128.49			120.04	119.73	119.56
GOR (cc/cc)	377.40	333.90	440.20	498.40	535.00			2648.0 0	2002.0 0	1838.0 0

TABLE 3
COMPARISON OF MULTICONTACT P-X AND BHS COMPOSITIONS

Component	Live Oil	D-44-F	Addition 6
N_2	0.0090	0.0124	0.0108
CO_2	0.0032	0.0012	0.0030
H_2S	0.0000	0.0000	0.0000
C_1	0.4578	0.6439	0.6386
C_2	0.1019	0.1146	0.0946
C_3	0.0749	0.0668	0.0627
i-C_4	0.0234	0.0157	0.0175
n-C_4	0.0369	0.0195	0.0261
i-C_5	0.0200	0.0088	0.0129
n-C_5	0.0215	0.0085	0.0132
C_6	0.0331	0.0128	0.0208
C_7	0.0246	0.0105	0.0122
C_8	0.0316	0.0131	0.0151
C_9	0.0188	0.0078	0.0088
C_{10}	0.0217	0.0087	0.0098
C_{11}	0.0167	0.0073	0.0076
C_{12}	0.0128	0.0054	0.0053
C_{13}	0.0111	0.0050	0.0049
C_{14}	0.0080	0.0039	0.0032
C_{15}	0.0065	0.0030	0.0025
C_{16}	0.0042	0.0020	0.0015
C_{17}	0.0033	0.0018	0.0013
C_{18}	0.0028	0.0014	0.0012
C_{19}	0.0020	0.0011	0.0009
C_{20}	0.0014	0.0008	0.0007
C_{21}	0.0011	0.0007	0.0006
C_{22}	0.0009	0.0006	0.0004
C_{23}	0.0008	0.0005	0.0003
C_{24}	0.0008	0.0004	0.0004
C_{25}	0.0006	0.0004	0.0003
C_{26}	0.0006	0.0003	0.0003
C_{27}	0.0006	0.0003	0.0003
C_{28}	0.0005	0.0003	0.0002
C_{29}	0.0005	0.0003	0.0002
C_{30+}	0.0011	0.0010	0.0004
CycloC_5	0.0025	0.0012	0.0012
MCycloC_5	0.0044	0.0020	0.0022
Benzene	0.0023	0.0007	0.0011
CycloC_6	0.0036	0.0017	0.0017
MCycloC_6	0.0098	0.0047	0.0047
Toluene	0.0061	0.0019	0.0030
o-Xylene	0.0029	0.0013	0.0013
1,2,4-Trimeth	0.0019	0.0011	0.0009
EB/MP-Xylene	0.0117	0.0047	0.0055
MW Recombined Oil	54.62	35.81	36.47
MW Separator Oil	128.40		124.88
GOR (cc/cc)	377.40	572	988.00

FIGURE 1
RELATIVE PORE SIZE DISTRIBUTION

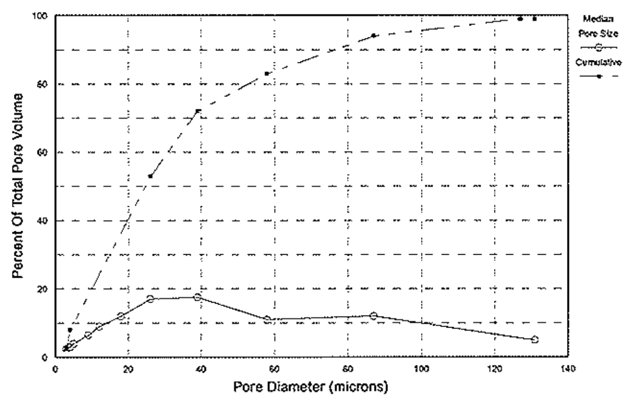

FIGURE 2
MMP PLOT

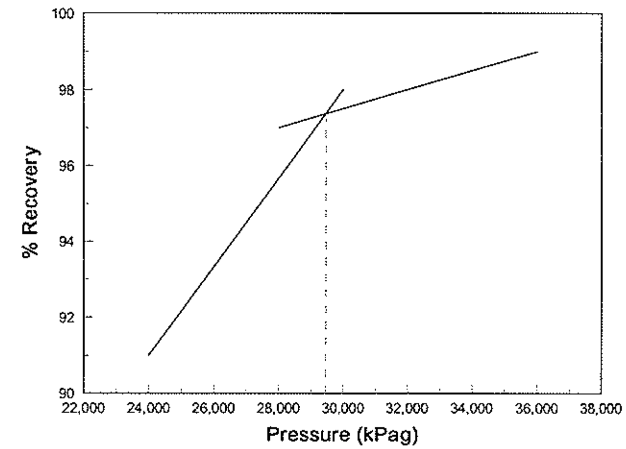

FIGURE 3

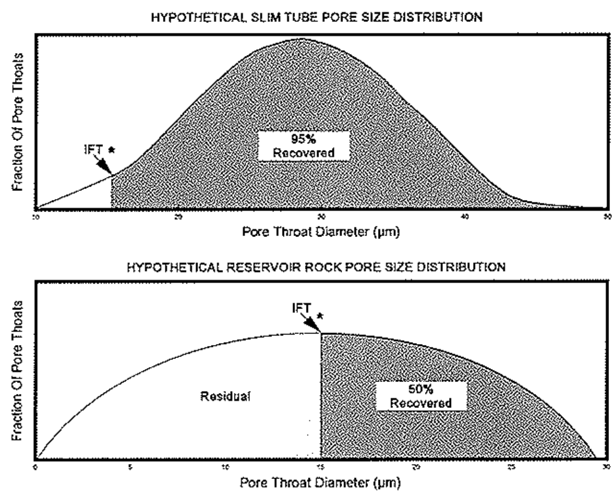

FIGURE 4
TERNARY PHASE LOOP

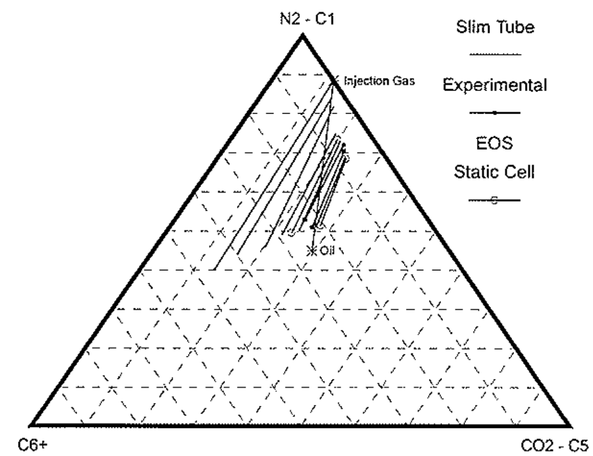

FIGURE 5
P-x DIAGRAMS
PRESSURE vs MOLE FRACTION SOLVENT ADDED

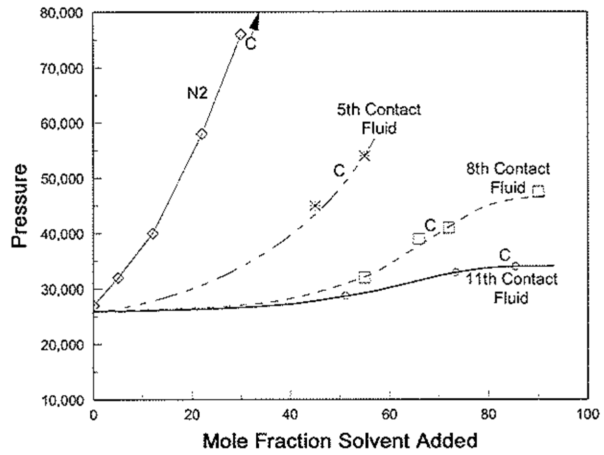

FIGURE 6
MOBILITY - DOMINATED SYSTEMS
RELATIVE PERMEABILITY vs SATURATION

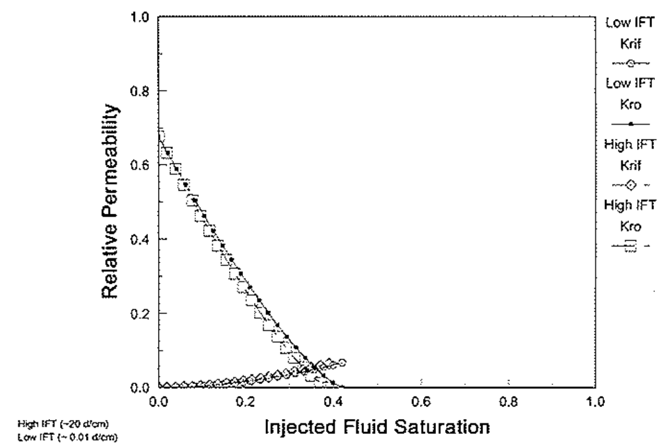

FIGURE 7
FORWARD AND REVERSE CONTACT
RELATIVE PERMEABILITY CURVES

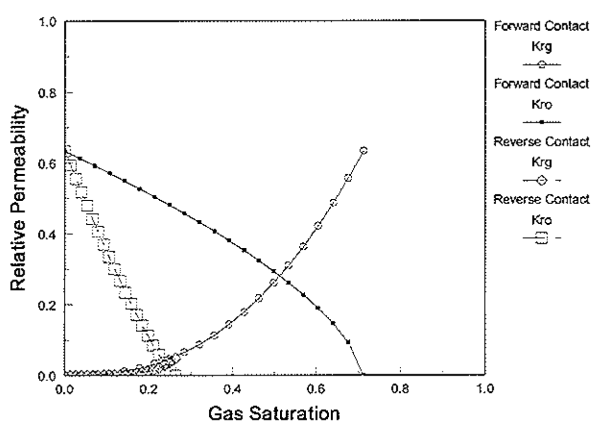

FIGURE 8
CONVENTIONAL & MULTICONTACT
P-x RESPONSE

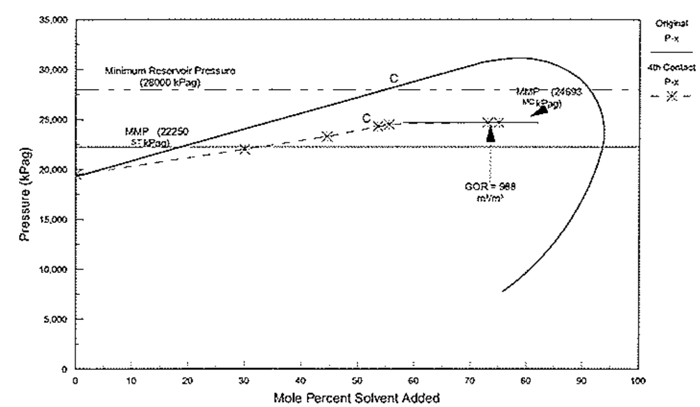

FIGURE 9
LOCATION MAP

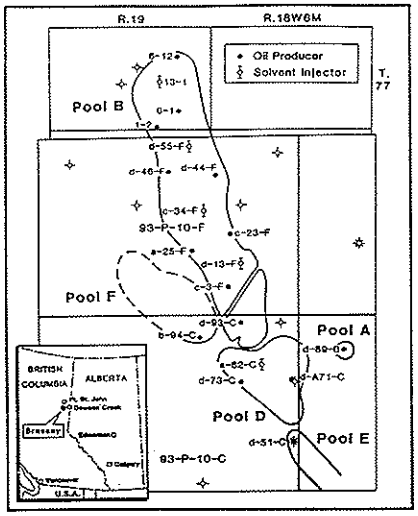

FIGURE 10
COMPARISON OF MULTICONTACT P-x AND BHS COMPOSITIONS

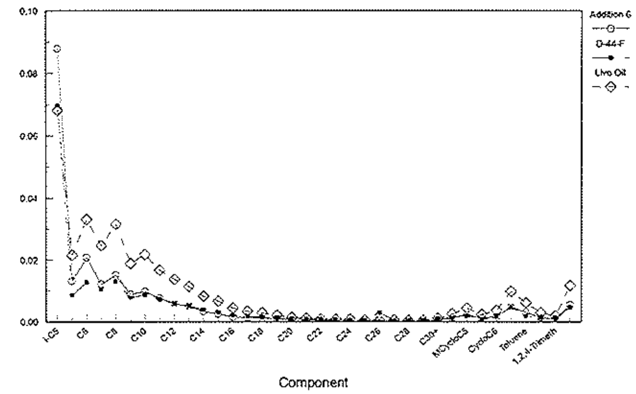

FIGURE 11
ENRICHMENT CORRELATION FOR
CASE HISTORY 2

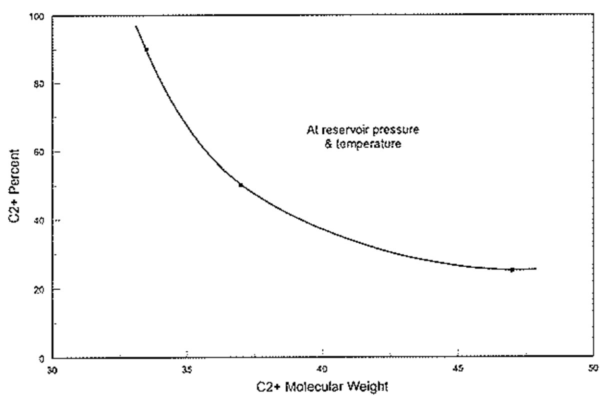

FIGURE 12
FIELD TRACER PROFILES